



## An analytic study of the magnetohydrodynamic stability of inverse shear profiles

C. G. Gimblett, R. J. Hastie, and T. C. Hender

Citation: *Phys. Plasmas* **3**, 3369 (1996); doi: 10.1063/1.871612

View online: <http://dx.doi.org/10.1063/1.871612>

View Table of Contents: <http://pop.aip.org/resource/1/PHPAEN/v3/i9>

Published by the [American Institute of Physics](#).

---

### Related Articles

Head-on-collision of modulated dust acoustic waves in strongly coupled dusty plasma

*Phys. Plasmas* **19**, 103708 (2012)

Effects of laser energy fluence on the onset and growth of the Rayleigh–Taylor instabilities and its influence on the topography of the Fe thin film grown in pulsed laser deposition facility

*Phys. Plasmas* **19**, 103504 (2012)

Halo formation and self-pinching of an electron beam undergoing the Weibel instability

*Phys. Plasmas* **19**, 103106 (2012)

Energy dynamics in a simulation of LAPD turbulence

*Phys. Plasmas* **19**, 102307 (2012)

Free boundary ballooning mode representation

*Phys. Plasmas* **19**, 102506 (2012)

---

### Additional information on Phys. Plasmas

Journal Homepage: <http://pop.aip.org/>

Journal Information: [http://pop.aip.org/about/about\\_the\\_journal](http://pop.aip.org/about/about_the_journal)

Top downloads: [http://pop.aip.org/features/most\\_downloaded](http://pop.aip.org/features/most_downloaded)

Information for Authors: <http://pop.aip.org/authors>

## ADVERTISEMENT

The advertisement features the 'AIP Advances' logo in green and yellow, with a series of yellow circles of varying sizes to its right. Below the logo, the text 'Special Topic Section: PHYSICS OF CANCER' is displayed in white on a dark green background. At the bottom, the phrase 'Why cancer? Why physics?' is written in yellow, and a blue button with the text 'View Articles Now' is positioned to the right.

AIP Advances

Special Topic Section:  
**PHYSICS OF CANCER**

Why cancer? Why physics? [View Articles Now](#)

# An analytic study of the magnetohydrodynamic stability of inverse shear profiles

C. G. Gimblett, R. J. Hastie, and T. C. Hender

UKAEA, Fusion (UKAEA/Euratom Fusion Association), Culham, Abingdon, Oxon, OX14 3DB, United Kingdom

(Received 16 January 1996; accepted 17 May 1996)

This paper reports on the ideal magnetohydrodynamic (MHD) stability of tokamak field profiles that have a non-monotonic safety factor  $q(r)$ . An analytic criterion is obtained for these ‘‘inverse shear’’ profiles by expanding in inverse aspect ratio and assuming that the minimum in  $q$  is slightly less than the  $m/n$  value of the mode under examination ( $m$  and  $n$  being the principal poloidal and toroidal mode numbers of the instability). Three terms are identified as controlling the stability of this ‘‘double kink’’; two of them are stabilizing and due, respectively, to field line bending and the interaction of average favorable curvature with the pressure gradient. The possibility of instability comes from the third term which is due to toroidal coupling and is ballooning in character. The analytic results are compared with those from a fully toroidal stability code.

[S1070-664X(96)00109-7]

## I. INTRODUCTION

The ‘‘inverse shear’’ mode of operation in magnetic fusion experiments<sup>1-5</sup> is a new confinement regime in which, by a sequence of setting-up procedures involving auxiliary heating or pellet injection during the current rise, a hollow current density profile is established in the device such that the safety factor profile  $q(r)$  is non-monotonic and typically exhibits a single off-axis minimum,  $q_{min}$ . Such a profile should be advantageous in stabilizing ideal ballooning modes<sup>6-9</sup> and certain classes of micro-instabilities such as the trapped electron mode.<sup>10,11</sup> Experimentally, particle and ion thermal diffusivities show a marked decrease and the latter can in fact drop to below the neoclassical value in the reversed shear region<sup>4</sup> with the resulting centrally peaked profiles enhancing the potential fusion power. An interesting development is that the improved confinement will produce significant bootstrap currents that, provided they are distributed correctly, could lead to steady state inverse shear operation, an exciting power plant prospect.<sup>12</sup>

Of course, the existence of the minimum in  $q$  brings into question the stability of global magnetohydrodynamic (MHD) instabilities such as the double tearing and, if the shear  $s=rq'/q$  in the core is small, the so-called ‘‘infernal’’ modes.<sup>13,14</sup> The latter exists purely because of toroidal coupling between the sideband poloidal harmonics generated by toroidicity, so any stability analysis must take this into account. In this paper we present an analytic stability analysis of inverse shear profiles in toroidal geometry. Introducing the inverse aspect ratio  $\epsilon (=a/R_0)$ , where  $a$  and  $R_0$  are the device minor and major radii, respectively, and the plasma  $\beta (=2\mu_0 p/B_0^2)$ , where  $p$  is the plasma pressure and  $B_0$  is the toroidal magnetic field, the calculations hinge on the assumption that the critical  $\beta/\epsilon$  is small, permitting the use of a low  $\beta$  expansion.<sup>15</sup> Further, we will require that the quantity  $(m/n - q_{min})$  [where  $(m,n)$  are the primary poloidal and toroidal mode numbers under investigation] is small, in a sense to be explained below (Sec. II).

The calculation is based on computing the ideal potential

energy  $\delta W$ .<sup>16</sup> A negative  $\delta W$  indicates the production of plasma kinetic energy, i.e., an unstable plasma. In cylindrical geometry,<sup>17</sup> the potential energy  $\delta W$  reduces to an integral between  $r_1$  and  $r_2$  where  $q(r_1)=q(r_2)=m/n$ . A ‘‘top-hat’’ radial displacement  $\xi_0$  in this region gives

$$\delta W_{cyl} = 2\pi^2 \frac{B_0^2}{R_0} \xi_0^2 \int_{r_1}^{r_2} r \left\{ (m^2 - 1) \left( \frac{1}{q} - \frac{n}{m} \right)^2 + \frac{2r\mu_0 p'}{B_0^2} \frac{n^2}{m^2} - \frac{2r^2}{R_0^2} \frac{n^2}{m^2} \left( \frac{1}{q^2} - \frac{n^2}{m^2} \right) \right\} dr, \quad (1)$$

where  $'$  represents the radial derivative. Thus, for  $(r_2 - r_1)/a \ll 1$ , expanding locally around the minimum of  $q$  we find

$$\frac{\delta W_{cyl}}{\xi_0^2} \propto \frac{8}{15} (m^2 - 1) \Delta^2 + \frac{2\mu_0 r p'}{B_0^2}, \quad (2)$$

where  $\Delta = (1 - nq_{min}/m)$ , and the destabilizing, pressure independent term which is of order  $\epsilon^2 \Delta$  has been dropped.<sup>17</sup> The positive first term on the right-hand side (rhs) of Eq. (2) represents the well-known stabilizing effect of field line bending, while the second (negative for normal monotonic decreasing pressure profiles) term is the cylindrical ‘‘Suydam’’<sup>18</sup> drive due to the destabilizing effect of the pressure gradient  $p'$  and field line curvature in a cylinder. Assuming the low  $\beta$  ordering  $\beta \sim O(\epsilon^2)$ , instability is predicted whenever  $\Delta \leq O(\epsilon)$ . So, instability can occur at  $\beta$  values for which pressure driven toroidal coupling to sideband harmonics cannot be ignored. This situation is analogous to the case of the  $(m,n)=(1,1)$  internal kink in the tokamak ordering,<sup>19</sup> where similar considerations apply.

The main result of this paper is to demonstrate that in a torus the  $\delta W$  produced by a similar displacement consists of three terms:

$$\frac{\delta W_{tor}}{\xi_0^2} \propto \frac{8}{15} (m^2 - 1) \Delta^2 + \frac{2\mu_0 r p'}{B_0^2} (1 - q_{min}^2) - \Lambda \alpha^2 \Delta^{1/2}. \quad (3)$$

The first term on the rhs of Eq. (3) again represents field line bending and is unchanged from the cylindrical calculation. Comparing the second term with its cylindrical counterpart we see that (for  $q_{min} > 1$ ) the favorable toroidal curvature converts the destabilizing cylindrical Suydam drive to a stabilizing (if  $q_{min} > 1$ ) Mercier<sup>20</sup> term. The third term, which gives the only possibility for instability, is a new ballooning destabilization. In Eq. (3),  $\Lambda$  is a number that encapsulates information regarding the coupling to toroidally induced sideband displacements  $\xi_1^{m \pm 1}$  with mode numbers  $(m \pm 1, n)$  (the  $\xi_1^{m \pm 1}$  extend across the minor radius  $a$  of the plasma), and  $\alpha = -(2\mu_0 R_0 \rho' q^2) / B_0^2$  is the well known parameter that controls the stability of high- $n$  ballooning modes.<sup>21</sup> The implications of Eq. (3) are discussed in Secs. II and V below.

In Sec. II we show how Eq. (3) is obtained. In Sec. III we deduce growth rates for these instabilities by matching the external MHD solutions to the solutions in the two inertial layers at  $r_1$  and  $r_2$ . In Sec. IV the analysis is validated by comparing the analytic growth rates with code results, and we conclude with a discussion in Sec. V.

## II. TOROIDAL ANALYSIS

The initial analysis follows that of Ref. 15. This reference addressed the problem of the stability of the  $(m, n) = (1, 1)$  mode in the case that  $|q - 1| \sim O(\epsilon = a/R)$  in the core region. Following the spirit of the procedure of Ref. 15 we assume the standard tokamak ordering and expand the plasma displacement  $\xi$  as  $\xi_0^m + \epsilon \xi_1^{(m \pm 1)} + \dots$  with

$$\xi_0^m = \xi_0(r) \exp(i(m\theta - n\phi)),$$

$\theta$  and  $\phi$  being poloidal and toroidal angles, respectively.

With these assumptions  $\delta W$  at first order can be minimized to zero by the choice

$$\frac{d}{dr}(r\xi_{0r}) + im\xi_{0\theta} = 0, \quad (4)$$

which eliminates the compressional Alfvén wave. If we then use  $\Delta \sim O(\epsilon)$  as part of the expansion, we arrive at second order with the analogue of Eq. (14) of Ref. 15,

$$\begin{aligned} \delta W_2 &= 2\pi^2 \frac{B_0^2}{R_0} \int_0^a r I(r) dr, \quad I = \sum_{j=1}^6 I_j, \\ I_1 &= \left(\frac{1}{q} - \frac{n}{m}\right)^2 \left[ r^2 \left(\frac{d\xi_0}{dr}\right)^2 + (m^2 - 1)\xi_0^2 \right], \\ I_2 &= \frac{\alpha^2 \xi_0^2}{2q^2}, \\ I_3 &= -r \frac{d\beta}{dr} \left(1 - \frac{1}{q^2}\right) \xi_0^2, \\ I_4 &= \frac{\alpha}{q^2} \left\{ q \left[ \xi_1^{(m+1)} + \xi_1^{(m-1)} \right] \frac{d}{dr} \left[ r \xi_0 \left( \frac{1}{q} - \frac{n}{m} \right) \right] \right. \\ &\quad \left. + \xi_0 \left( \xi_1^{(m+1)} + \xi_1^{(m-1)} \right) \right. \\ &\quad \left. + \xi_0 \left( 1 - \frac{nq}{m+1} \right) \frac{d}{dr} (r \xi_1^{(m+1)}) \right\}, \end{aligned} \quad (5)$$

$$+ \xi_0 \left( 1 - \frac{nq}{m-1} \right) \frac{d}{dr} (r \xi_1^{(m-1)}) \Big\},$$

$$I_5 = \left( \frac{1}{q} - \frac{n}{m+1} \right)^2 \left[ r^2 \left( \frac{d\xi_1^{(m+1)}}{dr} \right)^2 + m(m+2)\xi_1^{(m+1)2} \right],$$

$$I_6 = \left( \frac{1}{q} - \frac{n}{m-1} \right)^2 \left[ r^2 \left( \frac{d\xi_1^{(m-1)}}{dr} \right)^2 + m(m-2)\xi_1^{(m-1)2} \right],$$

where the scalar  $\xi$  functions refer to radial components.

We first note that the terms in  $I(r)$  that are quadratic in  $\xi_0$  are all stabilizing, and so a first minimization is clearly to take  $\xi_0(r) = 0$  in the regions  $0 < r < r_1$  and  $r_2 < r < a$  and we realize that it is only the coupling of  $\xi_0$  to its sidebands  $\xi_1^{(m \pm 1)}$ , as represented by  $I_4$ , that can provide the possibility of instability. In the regions  $0 < r < r_1$  and  $r_2 < r < a$  the Euler-Lagrange minimizing equations for  $\xi_1^{(m \pm 1)}(r)$  are the homogeneous cylindrical equations,<sup>15</sup>

$$\begin{aligned} \frac{d}{dr} \left[ r^3 \left( \frac{1}{q} - \frac{n}{m \pm 1} \right)^2 \frac{d\xi_1^{(m \pm 1)}}{dr} \right] \\ = m(m \pm 2) r \left( \frac{1}{q} - \frac{n}{m \pm 1} \right)^2 \xi_1^{(m \pm 1)}. \end{aligned} \quad (6)$$

We next form the Euler-Lagrange minimizing equations for these sidebands in the region  $r_1 < r < r_2$ . On rearranging the canonical form of these equations, and approximating the factor  $1/q - n/(m \pm 1)$  by  $\pm n/m(m \pm 1)$ , we find that they satisfy

$$\frac{d}{dr} \left[ r^{-2m-1} \frac{d}{dr} (\xi_1^{(m+1)} r^{2+m}) \right] = -\frac{(m+1)}{2} \frac{d}{dr} (\alpha r^{-m} \xi_0) \quad (7)$$

and

$$\frac{d}{dr} \left[ r^{2m-1} \frac{d}{dr} (\xi_1^{(m-1)} r^{2-m}) \right] = \frac{(m-1)}{2} \frac{d}{dr} (\alpha r^m \xi_0). \quad (8)$$

A notable feature of Eqs. (7) and (8) is that a first integral is clearly available. Before addressing this, we record the Euler-Lagrange minimizing equation for  $\xi_0$  in  $r_1 < r < r_2$ ,

$$\begin{aligned} \mathcal{L}(\xi_0) &\equiv \frac{d}{dr} \left[ r^3 \left( \frac{1}{q} - \frac{n}{m} \right)^2 \frac{d\xi_0}{dr} \right] - r \left[ (m^2 - 1) \left( \frac{1}{q} - \frac{n}{m} \right)^2 \right. \\ &\quad \left. + \frac{\alpha^2}{2q^2} - \frac{2r\mu_0 \rho'}{B_0^2} \left( 1 - \frac{1}{q^2} \right) \right] \xi_0 \\ &= \frac{\alpha r^{-m}}{2(m+1)q^2} \frac{d}{dr} [\xi_1^{(m+1)} r^{m+2}] \\ &\quad - \frac{\alpha r^m}{2(m-1)q^2} \frac{d}{dr} [\xi_1^{(m-1)} r^{2-m}]. \end{aligned} \quad (9)$$

Returning to Eqs. (7) and (8), first integrals are simply

$$\frac{d}{dr}(r^{m+2}\xi_1^{(m+1)}) = Ar^{1+2m} - \frac{(m+1)}{2}\alpha r^{m+1}\xi_0, \quad (10)$$

$$\frac{d}{dr}(r^{2-m}\xi_1^{(m-1)}) = Br^{1-2m} + \frac{(m-1)}{2}\alpha r^{-m+1}\xi_0, \quad (11)$$

with  $A$  and  $B$  as yet unknown constants. We note in passing that on substituting the relations (10) and (11) into the rhs of Eq. (9), the parts of the sidebands that are due to the direct  $\xi_0$  drive add together and have the effect of cancelling the term  $-r\alpha^2\xi_0/(2q^2)$  that appears on the left-hand side (lhs) of Eq. (9).

To proceed further, boundary conditions for Eqs. (10) and (11) can be found by integrating Eqs. (7) and (8) across  $r=r_1$  and, making use of the continuity of  $\xi_1^{(m\pm 1)}$  there [i.e.,  $\xi_1^{(m\pm 1)}(r_1-) = \xi_1^{(m\pm 1)}(r_1+)$ ] to find that

$$A = (2+m+b_{m+1})r_1^{-m}\xi_1^{(m+1)}(r_1) \quad (12)$$

and

$$B = (2-m+b_{m-1})r_1^m\xi_1^{(m-1)}(r_1). \quad (13)$$

Here we have introduced

$$b_{m\pm 1} = \frac{r_1}{\xi_1^{(m\pm 1)}(r_1)} \frac{d\xi_1^{(m\pm 1)}}{dr}(r_1-),$$

which is the value of this particular quantity obtained by solving Eq. (6) in the region  $0 < r < r_1$  [in the event that the  $(m+1)$  harmonic has a resonance at  $r_s^{(m+1)}$  in this region then Eq. (6) must be integrated in  $r_s^{(m+1)} < r < r_1$  using the ‘‘small’’ solution at  $r_s^{(m+1)22}$ ]. Similar considerations naturally apply at  $r=r_2$  and we can deduce

$$\xi_1^{(m\pm 1)}(r_2) = \left(\frac{r_2}{r_1}\right)^{\pm m} \left(\frac{2\pm m + b_{m\pm 1}}{2\pm m + c_{m\pm 1}}\right) \xi_1^{(m\pm 1)}(r_1), \quad (14)$$

where  $c_{m\pm 1}$  are the quantities analogous to  $b_{m\pm 1}$  for the outer region  $r_2 < r < a$ . We can now integrate Eq. (10) once more to find that

$$A = \left[ \frac{(m+1)^2(2+m+b_{m+1})(2+m+c_{m+1})}{(m-b_{m+1})(2+m+c_{m+1})r_1^{2(m+1)} - (m-c_{m+1})(2+m+b_{m+1})r_2^{2(m+1)}} \right] \int_{r_1}^{r_2} r^{m+1} \alpha \xi_0 dr. \quad (15)$$

Similarly,

$$B = \left[ \frac{(m-1)^2(2-m+b_{m-1})(2-m+c_{m-1})}{(m+c_{m-1})(2-m+b_{m-1})r_2^{2(1-m)} - (m+b_{m-1})(2-m+c_{m-1})r_1^{2(1-m)}} \right] \int_{r_1}^{r_2} r^{-m+1} \alpha \xi_0 dr. \quad (16)$$

With the  $\xi^{(m\pm 1)}$  sidebands satisfying their respective Euler-Lagrange equations (7) and (8), we find that  $\delta W_2$  is now given by

$$\delta W_2 = -2\pi^2 \frac{B_0^2}{R_0} \int_{r_1}^{r_2} \xi_0 \mathcal{L}(\xi_0) dr, \quad (17)$$

with  $\mathcal{L}(\xi_0)$  as given in Eq. (9). Collating all these results gives finally

$$\begin{aligned} \frac{R_0}{B_0^2} \frac{\delta W_2}{2\pi^2} = & \int_{r_1}^{r_2} r^3 \left(\frac{1}{q} - \frac{n}{m}\right)^2 \left(\frac{d\xi_0}{dr}\right)^2 dr + (m^2-1) \int_{r_1}^{r_2} r \left(\frac{1}{q} - \frac{n}{m}\right)^2 \xi_0^2 dr - \int_{r_1}^{r_2} 2r^2 \frac{\mu_0 P'}{B_0^2} \left(1 - \frac{1}{q^2}\right) \xi_0^2 dr - \Lambda_{(m+1)} \\ & \times \left\{ \int_{r_1}^{r_2} \left(\frac{r}{r_1}\right)^{m+1} \alpha \xi_0 dr \right\}^2 - \Lambda_{(m-1)} \left\{ \int_{r_1}^{r_2} \left(\frac{r}{r_1}\right)^{-m+1} \alpha \xi_0 dr \right\}^2, \end{aligned} \quad (18)$$

where

$$\Lambda_{(m+1)} = \frac{-n^2(m+1)(2+m+b_{m+1})(2+m+c_{m+1})}{2m^2[(m-b_{m+1})(2+m+c_{m+1}) - (m-c_{m+1})(2+m+b_{m+1})(r_2/r_1)^{2(m+1)}]}, \quad (19)$$

$$\Lambda_{(m-1)} = \frac{-n^2(m-1)(2-m+b_{m-1})(2-m+c_{m-1})}{2m^2[(m+b_{m-1})(2-m+c_{m-1}) - (m+c_{m-1})(2-m+b_{m-1})(r_2/r_1)^{2(1-m)}]}. \quad (20)$$

We can now identify the various terms in the expression (18), as discussed briefly in the Introduction. The first two terms on the rhs of Eq. (18) represent the stabilizing effect of field-line bending, while the third is the stabilizing Mercier term. The last two terms stem from the coupling to upper and

lower poloidal harmonic sidebands and provide the possibility of an instability ( $\delta W < 0$ ).

To produce a specific criterion, we introduce a ‘‘top-hat’’ trial function for  $\xi_0$ .<sup>17</sup> We will further expand around  $r_{min}$ , the radius at which  $q=q_{min}$ . Writing  $x$

$= (r - r_{min})/r_{min}$  we have

$$\begin{aligned} \left(\frac{1}{q} - \frac{n}{m}\right) &\sim \frac{1}{mq} \left(m - nq_{min} - \frac{nr_{min}^2 q'' x^2}{2}\right), \\ &= \frac{n^2}{m^2} \left(\frac{r_{min}^2 q''}{2}\right) \{\hat{\Delta} - x^2\}, \end{aligned} \quad (21)$$

where

$$\hat{\Delta} = \frac{2m}{nr_{min}^2 q''} \left(1 - \frac{nq_{min}}{m}\right) = \frac{2q}{r_{min}^2 q''} \Delta. \quad (22)$$

The integrals in Eq. (18) transform as

$$\int_{r_1}^{r_2} r dr \rightarrow 2r_{min}^2 \sqrt{\hat{\Delta}} \int_0^1 dy, \quad y = \frac{x}{\sqrt{\hat{\Delta}}}. \quad (23)$$

With  $\xi_0$  a top hat the first integral on the rhs of Eq. (18) vanishes. Evaluating the remaining integrals using Eqs. (21) and (23), and assuming  $m$  is sufficiently small so that we may take  $(r/r_1)^m \sim 1$  in  $[r_1, r_2]$  we arrive at

$$\begin{aligned} \delta W_2 &\propto \frac{8}{15} (m^2 - 1) \Delta^2 + \frac{2r_{min} \mu_0 p'}{B_0^2} (1 - q_{min}^2) \\ &\quad - \left(\frac{q_{min} \Delta}{2r_{min}^2 q''}\right)^{1/2} \Lambda \alpha^2, \end{aligned} \quad (24)$$

with

$$\begin{aligned} \Lambda &= \frac{(2 + m + b_{m+1})(2 + m + c_{m+1})}{(b_{m+1} - c_{m+1})} \\ &\quad + \frac{(2 - m + b_{m-1})(2 - m + c_{m-1})}{(b_{m-1} - c_{m-1})}. \end{aligned} \quad (25)$$

An immediate conclusion that can be drawn from Eq. (24) is that the system is stable (with this trial function for  $\xi_0$ ) when  $q_{min}$  is just below  $m/n$  (i.e.,  $\Delta \rightarrow 0$ ), as in this case the Mercier term dominates (provided  $q_{min} > 1$ ). On the other hand, when  $q_{min}$  is reduced [i.e.,  $\Delta \equiv (1 - nq_{min}/m)$  is increased], the field line bending terms will eventually dominate. Clearly there is a most unstable value of  $\Delta$ , which is obtainable by performing a simple minimization. In fact the most unstable  $\Delta$  is given by

$$\Delta = \left[ \frac{15\Lambda \alpha^2}{64(m^2 - 1)} \right]^{2/3} \left( \frac{2q_{min}}{r_{min}^2 q''} \right)^{1/3}. \quad (26)$$

We can now calculate  $\delta W_2(min)$  by inserting expression (26) into Eq. (24), and deduce a criterion for instability,

$$\begin{aligned} - \left( \frac{2r_{min} \mu_0 p'}{B_0^2} \right) &> 1.82 (m^2 - 1)^{1/5} \left( \frac{r_{min}}{R_0 q_{min}} \right)^{8/5} \\ &\quad \times \left( \frac{r_{min}^2 q''}{q_{min}} \right)^{2/5} \left( \frac{1}{\Lambda} \right)^{4/5} (q^2 - 1)^{3/5}. \end{aligned} \quad (27)$$

This gives a scaling for the critical  $\beta$  as  $O(\epsilon^{8/5})$  occurring at a  $\Delta$  that is  $O(\epsilon^{4/5})$  and  $(r_2 - r_1)/r_{min} \sim \sqrt{\Delta}$  which is  $O(\epsilon^{2/5})$ .

### III. CALCULATION OF GROWTH RATES

Calculation of ideal growth rates follows the general method of Ref. 16. The finite inertia of the plasma will lead to the creation of inertial layers at  $r_1$  and  $r_2$ . The sum of the kinetic ( $K$ ) and potential ( $W$ ) energies at either of these layers is given by

$$\begin{aligned} K + W &= 2\pi^2 \rho_0 R_0 \frac{\gamma^2}{m^2} \int_{layer} (1 + 2q^2) r \left( \frac{d\xi}{dr} \right)^2 dr \\ &\quad + \frac{B_0^2}{2\mu_0} \frac{1}{R_0} \int_{layer} \left( \frac{1}{q} - \frac{n}{m} \right)^2 r \left( \frac{d\xi}{dr} \right)^2 dr, \end{aligned} \quad (28)$$

and  $\xi$  will obey

$$\frac{d}{dr} \left\{ \left[ \frac{\gamma^2 (1 + 2q^2)}{\gamma_A^2 m^2} + \left( \frac{1}{q} - \frac{n}{m} \right)^2 \right] \frac{d\xi}{dr} \right\} = 0. \quad (29)$$

[In Eqs. (28) and (29)  $\rho_0$  is the plasma density,  $\gamma$  is the required growth rate, and  $\gamma_A$  is the Alfvén frequency  $B_0/(R_0 \sqrt{\mu_0 \rho_0})$ ; the term  $(1 + 2q^2)$  is an enhancement of the inertia due to toroidal effects.<sup>23</sup>] In this layer the displacement  $\xi_0(r)$  rises from 0 at  $r_1(-)$  to the value  $\xi_0$  at  $r_1(+)$ .

To proceed, at  $r_1$  we introduce a layer variable  $x = (r - r_1)/r_1$  and expand  $q$  locally as  $q = m/n + x r_1 q' [= m/n(1 + x s_1)]$  with the shear  $s_1 = r_1 q'/q$ . Integrating Eq. (29) once and substituting into Eq. (28) gives

$$\begin{aligned} W + K &= 2\pi^2 r_1^2 \frac{B_0^2}{\mu_0 R_0} \\ &\quad \times \xi_0^2 \left\{ \int_{-\infty}^{+\infty} \left[ \frac{\gamma^2 (1 + 2q^2)}{\gamma_A^2 m^2} + \frac{s_1^2}{q^2} x^2 \right]^{-1} dx \right\}^{-1}, \\ &= 2\pi r_1^2 \frac{B_0^2}{\mu_0 R_0} \xi_0^2 \left\{ \frac{|s_1| \sqrt{1 + 2q^2}}{q} \right\} \frac{\gamma}{\gamma_A}. \end{aligned} \quad (30)$$

A similar contribution will arise at  $r_2$ , and so

$$\frac{\gamma}{\gamma_A} = \frac{1}{2\pi} \frac{q}{\sqrt{1 + 2q^2}} \frac{\mu_0 R_0}{B_0^2} \frac{m}{(r_1^2 |s_1| + r_2^2 |s_2|)} \left( -\frac{\delta W}{\xi_0^2} \right) \quad (31)$$

[with  $\delta W$  as defined in Eq. (5)].

### IV. COMPARISON WITH CODE RESULTS

The growth rate [Eq. (31)] has been compared with results computed with the FAR resistive MHD code.<sup>24</sup> The FAR code solves the full resistive MHD equations in toroidal geometry with no ordering assumptions. To facilitate this comparison it was necessary to find conditions for which the assumed ordering is valid, in particular that  $\epsilon \beta_p \ll 1$ , implying a small Shafranov shift of the equilibrium.<sup>25</sup> In practice this resulted in using relatively extreme parameters to effect the comparison. An aspect ratio of 100 and a non-monotonic  $q$  profile varying between 2.95 on axis and 3.1 at the edge with a minimum of 1.974 was used, and the growth rates of the  $m=2$ ,  $n=1$  instability as predicted by the FAR code, and the above three coupled harmonic analysis, were compared as  $\beta_0$  was increased. The results of the comparison

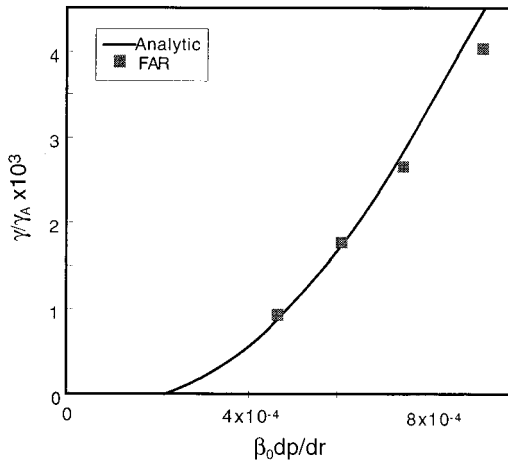


FIG. 1. Growth rate in poloidal Alfvén units against  $\beta_0 dp/dr$ . The pressure profile was taken to be  $\propto \Psi^2$  ( $\Psi$  is the poloidal flux function), and  $q = 2.95(1 + (r/1.2)^8)^{1/4} - 8.64r^2 e^{-15(r-0.25)^2}$ . The last FAR data point corresponds to  $\epsilon\beta_p = 0.16$ .

using these equilibrium parameters with a direct calculation of Eq. (31) is shown in Fig. 1 [for greater accuracy in calculating the  $\delta W$  of Eq. (31) we used the  $\Lambda_{(m \pm 1)}$  forms of Eqs. (18)–(20) rather than that of Eqs. (24)–(25)].

It can be seen that there is very good agreement between the analytic theory and the FAR computation. Further, examination of the eigenfunctions shows that  $\xi_0$  does have the assumed “top-hat” form between the two  $q=2$  radii.

## V. DISCUSSION AND CONCLUSIONS

We have presented an analytic study of the ideal MHD stability of inverse shear profiles, using an expansion in the inverse aspect ratio, coupled with the assumption that the minimum in the safety factor  $q_{min}$  is close to and less than the  $m/n$  value of the mode under consideration. This instability might be termed the pressure driven “double kink” mode. We have demonstrated that as the  $q$  profile evolves downwards:

- (i) For  $q_{min}$  very close to  $m/n$  [i.e.,  $\Delta = (1 - nq_{min}/m) \sim 0$ ], the Mercier favorable curvature dominates.
- (ii) The most unfavorable value of  $\Delta$  is  $O(\epsilon^{4/5})$ . For such a profile, pressure driven ballooning instability is possible at relatively low values of the local pressure gradient, corresponding to a global  $\beta$  which is  $O(\epsilon^{8/5})$ .
- (iii) For greater values of  $\Delta$ , the stabilizing field line bending effect dominates.
- (iv) The weak scaling of critical  $\beta$  with poloidal mode number  $m$  [ $\beta_{crit} \propto m^{2/5}$  in Eq. (27)] indicates that even high rational modes may be destabilized [e.g.,  $\beta_{crit}(m=10) \approx 2\beta_{crit}(m=2)$ ].

The analysis of this paper depends for its validity on an expansion of the tokamak equilibrium for large aspect ratio and weak Shafranov shift  $\Delta'_{Sh}(r) < 1$ . It is justified by the result that when  $q_{min}$  is just below a resonant value  $m/n$ , with  $(1 - nq_{min}/m) \sim \epsilon^{4/5}$ , the Shafranov shift is small [ $\Delta'_{Sh} \sim O(\epsilon^{3/5})$ ] at the marginally stable value of  $\beta$ . For such

an equilibrium the marginally stable MHD eigenmode can be adequately described by just three poloidal harmonics,  $m$  and  $m \pm 1$ . When  $q_{min}$  does not satisfy the ordering  $(1 - nq_{min}/m) \sim \epsilon^{4/5}$  marginal stability to ideal MHD modes occurs at higher  $\beta$  and the analytic methods employed in this calculation must fail to be accurate. The variation of the critical value of  $\beta_N$  as  $q_{min}$  is varied is clearly shown in the work of Phillips *et al.*<sup>26</sup> for several different  $m, n$  modes (e.g., Figs. 4 and 6–9 of Ref. 26). Thus Fig. 4 of Ref. 26 shows a distinct minimum in the critical value of  $\beta_N$  at values of  $q_{min}$  just below the corresponding rational value of  $m/n$ . So the qualitative feature of a local minimum of  $\beta_{crit}$  as a function of  $\Delta \equiv (1 - nq_{min}/m)$  persists at tight aspect ratio ( $A < 3$ ). Another limitation of the analytic calculations of this paper arises from the use of a trial function for  $\xi_0$  (the “top-hat” form) in evaluating Eq. (18). Comparison with the FAR code shows that the choice for  $\xi_0$  appears to be good close to marginal stability at the lowest  $\beta$  point. However, comparison with the  $\beta_N$  against  $q_{min}$  plots of Ref. 26 suggest that it becomes inadequate as  $q_{min} \rightarrow m/n$ .

This paper has only addressed the stability of equilibria with circular cross sections. However, as found in the analysis of the internal kink mode,<sup>27,28</sup> shaping of the cross section will drive additional poloidal harmonics in the eigenfunction. In the case of elliptic shaping these harmonics give rise to additional contributions to the energy integral of Eq. (3) that are quadratic in the ellipticity. A second shaping effect arises because of the direct coupling of the toroidal sideband harmonics by the ellipticity. As a result of this Eq. (3) will also contain a contribution linear in the ellipticity. The coefficients of these terms will, like  $\Lambda$ , depend on the details of the  $q(r)$  profile. So it appears that the effect of ellipticity will depend on the orientation (horizontal or vertical) of the elongation. Work is underway to determine the sign and amplitude of these effects and will be reported in a later paper.

## ACKNOWLEDGMENTS

We thank Dr. J. Manickam and colleagues at the Princeton Plasma Physics Laboratory for discussions on inverse shear issues, and Dr. M. Hughes for providing a preprint of Ref. 26.

This work was funded jointly by the U.K. Department of Trade and Industry and Euratom.

<sup>1</sup>M. Hugon, B. Ph. van Milligen, P. Smeulders, L. C. Appel, D. V. Bartlett, D. Boucher, A. W. Edwards, L.-G. Eriksson, C. W. Gowers, T. C. Hender, G. Huysmans, J. J. Jacquinot, P. Kupschus, L. Porte, P. H. Rebut, D. F. H. Start, F. Tibone, B. J. D. Tubbing, M. L. Watkins, and W. Zwingmann, Nucl. Fusion **32**, 33 (1992).

<sup>2</sup>G. T. Hoang, C. Gil, E. Joffrin, D. Moreau, A. Becoulet, P. Bibet, J. P. Bizarro, R. V. Budny, J. Carrasco, J. P. Coulon, C. De Michelis, T. Dudok de Wit, P. Monier-Garbet, M. Goniche, R. Guirlet, T. Hutter, S. M. Kaye, J. Lasalle, L. Laurent, P. Lecoustey, X. Litaudon, M. Mattioli, Y. Peysson, A.-L. Pecquet, G. Rey, S. A. Sabbagh, B. Saoutic, G. Tonon, and J. C. Vallet, Nucl. Fusion **34**, 75 (1994).

<sup>3</sup>Y. Kamada, K. Ushigusa, O. Naito, Y. Neyatani, T. Ozeki, K. Tobita, S. Ishida, R. Yoshino, M. Kikuchi, M. Mori, and H. Ninomiya, Nucl. Fusion **34**, 1605 (1994).

<sup>4</sup>F. M. Levinton, M. C. Zarnstorff, S. H. Batha, M. Bell, R. E. Bell, R. V. Budny, C. Bush, Z. Chang, E. Fredrickson, A. Janos, J. Manickam, A. Ramsey, S. A. Sabbagh, G. L. Schmidt, E. J. Synakowski, and G. Taylor, Phys. Rev. Lett. **75**, 4417 (1995).

- <sup>5</sup>E. J. Strait, L. L. Lao, M. E. Mauel, B. W. Rice, T. S. Taylor, K. H. Burrell, M. S. Chu, E. A. Lazarus, T. H. Osborne, S. J. Thompson, and A. D. Turnbull, *Phys. Rev. Lett.* **75**, 4421 (1995).
- <sup>6</sup>J. W. Connor, R. J. Hastie, and J. B. Taylor, *Proc. R. Soc. London Ser. A* **365**, 1 (1979).
- <sup>7</sup>A. Sykes, J. A. Wesson, and S. J. Cox, *Phys. Rev. Lett.* **39**, 757 (1977).
- <sup>8</sup>P. Smeulders, L. C. Appel, B. Balet, T. C. Hender, L. Lauro-Taroni, D. Stork, B. Wolle, S. Ali-Arshad, B. Alper, H. J. De Blank, M. Bureš, B. De Esch, R. Gianelli, R. König, P. Kupschus, K. Lawson, F. B. Marcus, M. Mattioli, H. W. Morsi, D. P. O'Brien, J. O'Rourke, G. J. Sadler, G. L. Schmidt, P. M. Stubberfield, and W. Zwingmann, *Nucl. Fusion* **35**, 225 (1995).
- <sup>9</sup>J. M. Greene and M. S. Chance, *Nucl. Fusion* **21**, 453 (1981).
- <sup>10</sup>B. B. Kadomtsev and O. P. Pogutse, *JETP* **24**, 1172 (1967).
- <sup>11</sup>G. Rewoldt, W. M. Tang, J. Manickam, and C. Kessel, in *Local Transport Studies in Fusion Plasmas*, edited by J. D. Callen, G. Gorini, and E. Sindoni, International School of Plasma Physics "Piero Caldirola" (Società Italiana di Fisica, Varenna, 1993), p. 333.
- <sup>12</sup>R. J. Goldston, S. H. Batha, R. H. Bulmer, D. N. Hill, A. W. Hyatt, S. C. Jardin, F. M. Levinton, S. M. Kaye, C. E. Kessel, E. A. Lazaros, J. Manickam, G. H. Nielsen, W. M. Nevins, L. J. Perkins, G. Rewoldt, K. I. Thomassen, M. C. Zarnstorff, and the National TPX Physics Team, *Plasma Phys. Controlled Fusion* **36**, B213 (1994).
- <sup>13</sup>J. Manickam, N. Pomphrey, and A. M. M. Todd, *Nucl. Fusion* **27**, 1461 (1987).
- <sup>14</sup>L. A. Charlton, R. J. Hastie, and T. C. Hender, *Phys. Fluids B* **1**, 798 (1989).
- <sup>15</sup>R. J. Hastie and T. C. Hender, *Nucl. Fusion* **28**, 585 (1988).
- <sup>16</sup>I. B. Bernstein, E. A. Frieman, M. D. Kruskal, and R. M. Kulsrud, *Proc. R. Soc. London Ser. A* **244**, 17 (1958).
- <sup>17</sup>H. P. Furth, P. H. Rutherford, and H. Selberg, *Phys. Fluids* **16**, 1054 (1973).
- <sup>18</sup>B. R. Suydam in *Proceedings of the Second U.N. International Conference on the Peaceful Uses of Atomic Energy*, Geneva, 1958 [Columbia University Press, (I.D.S.), New York, 1959], Vol. 31, p. 157.
- <sup>19</sup>M. N. Bussac, R. Pellat, D. Edery, and J. L. Soulé, *Phys. Rev. Lett.* **35**, 1638 (1975).
- <sup>20</sup>C. Mercier, *Nucl. Fusion Suppl. Pt. 2*, 801 (1962); J. M. Greene and J. L. Johnson, *Phys. Fluids* **5**, 510 (1962).
- <sup>21</sup>J. W. Connor, R. J. Hastie, and J. B. Taylor, *Phys. Rev. Lett.* **40**, 396 (1978).
- <sup>22</sup>J. W. Connor, S. C. Cowley, R. J. Hastie, T. C. Hender, A. Hood, and T. J. Martin, *Phys. Fluids* **31**, 577 (1988).
- <sup>23</sup>A. H. Glasser, J. M. Greene, and J. L. Johnson, *Phys. Fluids* **18**, 875 (1975).
- <sup>24</sup>L. A. Charlton, J. A. Holmes, H. R. Hicks, V. E. Lynch, and B. A. Carreras, *J. Comput. Phys.* **63**, 107 (1986).
- <sup>25</sup>J. A. Wesson, *Tokamaks* (Clarendon, Oxford, 1987).
- <sup>26</sup>M. W. Phillips, M. C. Zarnstorff, J. Manickam, F. M. Levinton, and M. H. Hughes, *Phys. Plasmas* **3**, 1673 (1996).
- <sup>27</sup>D. Edery, G. Laval, R. Pellat, and J. L. Soulé, *Phys. Rev. Lett.* **19**, 260 (1976).
- <sup>28</sup>See AIP Document No. PAPS PFLDA-30-1756-36 for 36 pages of "The effect of shaped plasma cross sections on the ideal internal kink mode in a tokamak" by J. W. Connor and R. J. Hastie (Culham Laboratory Report No. CLM-M106, 1985). Order by PAPS number and journal reference from American Institute of Physics, Physics Auxiliary Publication Service, Carolyn Gehlbach, 500 Sunnyside Blvd., Woodbury, NY 11797-2999. Fax 516-576-2223, e-mail: paps@aip.org. The price is \$1.50 for each microfiche (98 pages) or \$5.00 for photocopies of up to 30 pages, and \$0.15 for each additional page over 30 pages. Airmail additional. Make checks payable to the American Institute of Physics.